

# MicroRNA-19a-3p inhibits the cellular proliferation and invasion of non-small cell lung cancer by downregulating UBAP2L

YUEJIANG PAN, KE JIN, XUAN XIE, KEXI WANG and HUIZHONG ZHANG

Guangdong Provincial Key Laboratory of Malignant Tumor Epigenetics and Gene Regulation,  
Sun Yat-sen Memorial Hospital, Sun Yat-sen University, Guangzhou, Guangdong 510120, P.R. China

Received March 14, 2018; Accepted August 15, 2018

DOI: 10.3892/etm.2020.8926

**Abstract.** MicroRNAs (miRNAs) are increasingly recognized as important regulators of non-small cell lung cancer (NSCLC) progression by directly regulating their target genes. The aim of the present study was to assess the biological role of miR-19a-3p in NSCLC. It was revealed that miR-19a-3p expression was significantly downregulated in human NSCLC tissues and cell lines compared with normal tissues and lung epithelial cells. In addition, a lower miR-19a-3p expression was significantly associated with Tumor Node Metastasis stage and lymph node metastasis. Furthermore, the upregulation of miR-19a-3p in NSCLC cell lines significantly inhibited cell proliferation, migration and invasion, as determined using an MTT, colony formation, wound healing and transwell Matrigel invasion assays, respectively. A luciferase reporter assay and western blotting determined that ubiquitin associated protein 2 like (UBAP2L) was a direct target of miR-19a-3p and could be inhibited through the upregulation of miR-19a-3p in NSCLC. In addition, UBAP2L silencing induced similar effects to those observed following miR-19a-3p overexpression. The overexpression of UBAP2L partially reversed the effects of miR-19a-3p on NSCLC cell lines. Collectively, these data indicated that miR-19a-3p may serve as a tumor suppressor partly through the regulation of UBAP2L expression in NSCLC and that the targeting of miR-19a-3p may be a novel method for NSCLC treatment.

## Introduction

Lung cancer is a common malignancy in men and women worldwide, that was estimated to cause 162,510 new cases and 595,690 cases of mortality in the United States in 2016 (1). As

the primary histological subtype of lung cancer, non-small-cell lung cancer (NSCLC) comprises ~85% cases of lung cancer (2). Several critical risk factors, including smoking, asbestos, arsenic, genetics and epigenetics have been identified to be responsible for NSCLC development (3). The current therapeutic treatments used for patients with NSCLC include surgery, chemotherapy, radiotherapy, epidermal growth factor receptor inhibitors and anaplastic lymphoma kinase inhibitors (4,5). Despite improvement in these therapies, the 5-year overall survival rate is only 16% for all stages (6). Therefore, the elucidation of the molecular mechanism underlying NSCLC carcinogenesis for the early diagnosis and treatment of NSCLC is required.

MicroRNAs (miRNAs or miRs) are comprised of 20-23 nucleotide duplexes that post-transcriptionally regulate gene expression in a wide variety of eukaryotic organisms (7). Single-stranded miRNAs bind to 'seedless' 3'untranslated regions (3'UTR) of their target mRNA, which causes a decrease in its translation (8). Previous studies have demonstrated that miRNAs participate in multiple cellular processes, including early development, proliferation, apoptosis, cell death, fat metabolism and differentiation (9-11). The alterations of miRNA profiles have been confirmed in various types of human malignancies, including lung, breast, gastric, leukemia and liver cancer (8,12). As a member of the miR-17-92 cluster, miR-19a-3p has been demonstrated to be downregulated in prostate cancer, but overexpressed in myeloma and breast cancer (13,14), indicating that it is a regulator of tumor growth, progression and metastasis. However, whether it serves a primary role in the development and progression of NSCLC remains unclear.

Ubiquitin associated protein 2 like (UBAP2L) is a novel B lymphoma Mo-MLV insertion region 1-interacting protein with a ubiquitin-associated domain and RGG/RG motif that has also been demonstrated to participate in the maintenance of hematopoietic stem cell activity and mitosis by regulating kinetochore-microtubule attachment (15). Previous studies have assessed the role of UBAP2L in the expression and tumorigenesis of prostate cancer (16), glioma (17), hepatocellular carcinoma (18), colorectal carcinoma and breast cancer (19). UBAP2L has also been suggested to regulate certain physiological and pathophysiological processes of malignant tumors by accelerating epithelial-mesenchymal transition (EMT), proliferation, migration and G2/M phase transition, as well as

*Correspondence to:* Mr. Huizhong Zhang, Guangdong Provincial Key Laboratory of Malignant Tumor Epigenetics and Gene Regulation, Sun Yat-sen Memorial Hospital, Sun Yat-sen University, 107 Yan Jiang West Road, Guangzhou, Guangdong 510120, P.R. China  
E-mail: zhhzhgd\_2008@163.com

**Key words:** microRNA-19a-3p, ubiquitin associated protein 2 like, non-small cell lung cancer, cell proliferation, migration, invasion

inhibiting apoptosis in cancer cells (16,17,20). Furthermore, Aucagne *et al* (21) demonstrated that ~15% of human primary lung adenocarcinoma specimens exhibit a high UBAP2L expression and that UBAP2L amplification contributes to EMT in NSCLC cells.

In view of the fact that miR-19a-3p is frequently altered in several types of cancer cells, the present study hypothesized that it may participate in NSCLC progression. Therefore, miR-19a-3p expression was assessed in NSCLC tissues and cells, and its biological function in tumor cell proliferation, colony formation and migration were further determined using the gain-of-function approach. In addition, the current study assessed the association between miR-19a-3p and UBAP2L, and determined their impact on NSCLC cell progression. The results revealed a novel mechanism of miR-19a-3p in lung cancer and indicated a potential for its novel use in miR-19a-3p-based therapeutic development.

## Materials and methods

**Human NSCLC tissue samples.** A total of 75 paired patient samples of NSCLC tissues and matched adjacent noncancerous tissues (5 cm from tumor edge) were obtained in Sun Yat-sen Memorial Hospital (Guangzhou, China) from December 2014 to September 2016. Tissue samples were acquired during routine therapeutic surgery of patients with NSCLC who did not receive chemotherapy, radiotherapy or other systemic treatments prior to surgery. All tissues were immediately snap-frozen in liquid nitrogen and stored at -80°C. Specific details of the patients included in the present study are summarized in Table I. Prior to enrollment, all patients with NSCLC provided their signed written informed consent for the use of their tissue. The current study was approved by the Ethics Committee of Sun Yat-sen Memorial Hospital (approval no. sm20163254).

**Cell culture and transfection.** The human NSCLC cell lines (A549, H1650, SPC-A1, and H1299) and one human normal bronchial epithelial cell line BEAS-2B were obtained from the American Type Culture Collection (Manassas, VA, USA). A549, H1299 and H1650 cells were cultured in RPMI-1640 medium (Gibco; Thermo Fisher Scientific, Inc., Waltham, MA, USA). SPC-A1 and BEAS-2B cell lines were cultivated in Dulbecco's Modified Eagle's Medium (DMEM; Gibco; Thermo Fisher Scientific, Inc.). All cell lines were maintained in 90% media supplemented with 10% fetal bovine serum (FBS; Gibco; Thermo Fisher Scientific, Inc.) in a 5% CO<sub>2</sub> humidified environment at 37°C.

miR-19a-3p mimics, small interfering (si)RNA for UBAP2L (siUBAP2L, cat. no. 3624), the UBAP2L overexpression plasmid (pcDNA3.1-UBAP2L; cat. no. 1302) and their corresponding negative controls (NC; cat. no. 4126; miR-NC; cat. no. 3106, siNC; cat. no. 2036 and pcDNA3.1; cat. no. 1987, respectively) were purchased from Shanghai GenePharma Co., Ltd., (Shanghai, China). For cell transfection, cells were dissociated into single cells and transfected with 30 nM of miR-19a-3p mimics or negative control mimics. For UBAP2L knockdown, A549 cells were transfected with 30 nM siUBAP2L or siNC. In rescue experiments, cells were co-transfected with 30 nM miR-19a-3p mimics together with

10 µg pcDNA3.1 or pcDNA3.1-UBAP2L at the same time. All cell transfections were performed using Lipofectamine® 2000 (Invitrogen; Thermo Fisher Scientific, Inc.) according to the manufacturer's protocol. A total of 6 h following transfection, transfection media were replaced with culture media. Cells were harvested for subsequent experimentation 48 h post-transfection.

**Reverse transcription-quantitative polymerase chain reaction (RT-qPCR).** Total RNA was isolated from tissue or cell samples using TRIzol reagent (Invitrogen; Thermo Fisher Scientific, Inc.) according to manufacturer's protocol. A NanoDrop ND-1000 spectrophotometer (NanoDrop Technologies; Thermo Fisher Scientific, Inc.) was used to measure RNA quality and quantity. Total RNA was reverse transcribed into cDNA using the M-MLV Reverse Transcriptase kit (Promega Corporation, Madison, WI, USA) and used to analyze the expression of miR-19a-3p and UBAP2L. For miR-19a-3p detection, the expression of miR-19a-3p was determined by qPCR using the miScript SYBR Green PCR kit (Qiagen China Co., Ltd., Shanghai, China) with miR-19a-3p-specific primers (forward, 5'-TGCAATGTGTGTGTAGCCA-3' and reverse, 5'-ATCATTGCTCCTTGGATGGT-3'). For UBAP2L mRNA expression, qPCR was performed using Power SYBR Green RT-PCR Reagent kit (Invitrogen; Thermo Fisher Scientific, Inc.) and the ABI7500 system (Applied Biosystems; Thermo Fisher Scientific, Inc.) with paired UBAP2L primers (forward, 5'-ACACAATCCCCATCACTGGT-3' and reverse, 5'-CAGAGGAGAAGACGGAGGTG-3'). The following thermocycling conditions were used for qPCR: Initial denaturation at 95°C for 10 min; 40 cycles of 95°C for 10 sec. The relative miR-19a-3p and UBAP2L expression levels were determined using the 2<sup>-ΔΔC<sub>q</sub></sup> method (22) and normalized to U6 (forward, 5'-GCTCGCTTCGGCAGCACA-3' and reverse, 5'-GAGGTA TTGCACCAAGAGGA-3') and β-actin (forward, 5'-TCTCTG CTCTCCCTGTTCT-3' and reverse, 5'-ATCCGTTTACAC CGACCTTC-3'), respectively.

**MTT assay.** An MTT assay was performed to assess NSCLC cell proliferation. A549/H1299 cells were seeded into 96-well plates at a density of 3x10<sup>3</sup> cells/well and incubated for 0, 24, 48, 72 or 96 h at 37°C. MTT (5 mg/ml; 20 µl) was added to each well and incubated for an additional 4 h at 37°C. Following the removal of supernatant, 100 µl DMSO (Sigma-Aldrich; Merck KGaA, Darmstadt, Germany) was added to each well to stop the reaction. Absorbance was detected at a wavelength of 595 nm using a microplate reader (Bio-Rad Laboratories, Inc., Hercules, CA, USA).

**Colony formation assay.** A549 cells were seeded in 6-well plates at a density of 600 cells/well and incubated at 37°C for 14 days. Colonies were fixed with 4% PFA for 10 min at room temperature and stained with crystal violet (0.5% w/v) for 20 min at room temperature. Cell colonies containing at least 50 cells were counted and imaged under a light microscope (magnification, x200).

**Wound healing assay.** Cell migration was assessed using a wound healing assay in A549 and H1299 cell lines. Cells were seeded onto 6-well plates (2x10<sup>5</sup> cells/well) following

Table I. Association between miR-19a-3p expression and clinicopathological characteristics in patients with NSCLC (n=75).

Patient characteristics	Cases (n=75)	Expression of miR-19a-3p		P-value (chi-squared test)
		Low (n=46)	High (n=29)	
Sex				0.712
Male	41	26	15	
Female	34	20	14	
Age (years)				0.432
<60	38	21	17	
≥60	37	25	12	
Tumor size (cm)				0.451
<4	49	29	20	
≥4	26	17	9	
Histological grade				0.278
Well/moderate	47	31	16	
Poor	28	15	13	
TNM stage				0.013 <sup>a</sup>
I+II	55	29	26	
III+IV	20	17	3	
Lymph node metastasis				0.021 <sup>a</sup>
Negative	49	26	23	
Positive	26	20	6	

TNM, tumor, node, metastasis; miR, miRNA. <sup>a</sup>P<0.05.

transfection and cultured for 24 h at 37°C. A wound field was then made using a sterile 200 µl pipette tip through the cell layer in each well. Subsequently, representative images at 0 and 48 h following wounding were captured under a light microscope (magnification, x200). Wound healing rate was determined by measuring the distance of migrating cells from five different areas of each wound according to a previous study (23).

**Transwell Matrigel invasion assay.** A 24-well Transwell chamber (pore size, 8.0 µm; Corning Inc., Corning, NY, USA) was pre-coated with BD Matrigel® (BD Biosciences, Franklin Lakes, NJ, USA). A total of 4x10<sup>4</sup> transfected cells were cultured in serum-free DMEM medium and subsequently placed into the upper chamber. In the lower chamber, DMEM medium supplemented with 10% FBS was added as a chemoattractant. Following 48-h incubation at 37°C, the medium was removed from the upper chamber and the cells on the lower surface were fixed with 4% methanol for 10 min at room temperature and stained with 0.1% crystal violet for 5 min at room temperature. Migratory cells were observed in five randomly selected fields under a light microscope (magnification, x200).

**Target prediction and dual reporter luciferase assay.** The online miRDB (www.mirdb.org), miRanda (www.microrna.org) and TargetScan (www.targetscan.org) databases were used to predict the direct targets of miR-19a-3p. Among the predicted targeted genes, UBAP2L was selected as it functions

as a tumor gene in several types of cancer, including breast cancer (19) and hepatocellular carcinoma (18). For the dual reporter luciferase assay, the 3'UTR of UBAP2L was cloned into the psiCHECK-2 luciferase reporter vector (Promega Corporation) and named the wild type (UBAP2L WT). Site-directed mutagenesis of the miR-19a-3p binding site in the UBAP2L 3'UTR was performed using the GeneTailor Site-Directed Mutagenesis System (Invitrogen; Thermo Fisher Scientific, Inc.). Similarly, the 3'UTR of UBAP2L containing the mutated binding region was cloned into the aforementioned vector and called the mutated-type (UBAP2L MUT). Cells (2x10<sup>5</sup> per well) were seeded in 24-well plates and co-transfected with UBAP2L WT or UBAP2L MUT together with the miR-19a-3p mimic or the miR-NC using the Lipofectamine® 2000 reagent at 37°C in triplicate. Cells were harvested 48 h following co-transfection. Firefly and *Renilla* luciferase activities were measured using the Dual-Luciferase Reporter Assay kit (Promega Corporation) according to the manufacturer's protocol.

**Western blot analysis.** Transfected cells were harvested and total protein was extracted using radioimmunoprecipitation lysis buffer (Beyotime Institute of Biotechnology, Haimen, China). Following centrifugation at 12,000 x g for 15 min at 4°C, total protein was quantified using a bicinchoninic acid protein assay kit (Beyotime Institute of Biotechnology). Subsequently, 30 µg protein/lane was separated via SDS-PAGE on a 10% gel. The separated proteins were transferred to polyvinylidene difluoride membranes (EMD Millipore, Billerica, MA, USA)

and blocked for 1 h at room temperature with 5% skimmed milk. The membranes were incubated with primary antibodies against UBAP2L (1:1,000; cat. no. ab70319; Abcam, Cambridge, UK) or GAPDH (1:50,000; cat. no. 10494-1-AP; ProteinTech Group, Inc., Chicago, IL, USA) overnight at 4°C. Membranes were washed three times with Tris-buffered saline containing 0.5% Tween-20. Following primary incubation, membranes were incubated with goat anti-rabbit immunoglobulin G horse-radish peroxidase-conjugated secondary antibodies (1:5,000; cat. no. sc-2054; Santa Cruz Biotechnology, Inc., Dallas, TX, USA) for 2 h at room temperature. Protein bands were visualized using an enhanced chemiluminescence detection kit (Pierce; Thermo Fisher Scientific, Inc.) and GAPDH was used as an internal control.

**Statistical analysis.** All statistical analyses were performed using SPSS software (version 17.0; SPSS, Inc., Chicago, IL, USA). Experimental data were presented as the mean  $\pm$  standard deviation. Chi-squared test was used to analyze miR-19a-3p expression and the patient characteristics of NSCLC tissues. The differences in miR-19a-3p expression between tumor and adjacent tissues were evaluated using a paired Student's t-test. Pearson's correlation coefficient was utilized to determine the correlation between miR-19a-3p and UBAP2L expression in NSCLC tissues using GraphPad Prism 6.0 software (GraphPad Software, Inc., La Jolla, CA, USA). The differences between two groups were assessed using Student's t-test. One-way analysis of variance followed by Tukey's post-hoc test was used to measure the significance of comparisons between multiple groups.  $P < 0.05$  was considered to indicate a statistically significant result.

## Results

**MiR-19a-3p expression in NSCLC tissues and cell lines, and its association with the clinicopathological features of patients with NSCLC.** To assess the biological role of miR-19a-3p in NSCLC, the expression levels of miR-19a-3p were first determined using RT-qPCR in 75 paired patient samples of NSCLC tissues and matched adjacent noncancerous tissues. As presented in Fig. 1A, the expression of miR-19a-3p in tumor tissue was significantly downregulated compared with matched adjacent noncancerous tissues ( $P < 0.0001$ ). The association between clinicopathological characteristics and miR-19a-3p expression in patients with NSCLC was subsequently determined. All samples were divided into high and low miRNA expression, according to the median miR-19a-3p expression value. As presented in Table I, low miR-19a-3p expression was significantly associated with TNM stage ( $P = 0.013$ ) and lymph node metastasis ( $P = 0.021$ ), whereas no statistical differences was identified with sex ( $P = 0.712$ ), age ( $P = 0.432$ ), tumor size ( $P = 0.451$ ) and histological grade ( $P = 0.278$ ). The expression of miR-19a-3p in NSCLC cell lines was also assessed. It was demonstrated that miR-19a-3p was significantly downregulated in A549, H1650, SPC-A1 and H1299 cells compared with BEAS-2B cells (Fig. 1B;  $P < 0.01$  and  $P < 0.001$ ).

**MiR-19a-3p overexpression inhibits cell proliferation in NSCLC.** To elucidate the biological function of miR-19a-3p in NSCLC *in vitro*, A549 and H1299 cells with a relatively

low miR-19a-3p expression were selected for gain-of-function assays. As presented in Fig. 2A, RT-qPCR results confirmed that miR-19a-3p levels increased significantly in A549 and H1299 cells transfected with miR-19a-3p mimics compared with scrambled miR-NCs (both  $P < 0.01$ ). The effect of miR-19a-3p on cell proliferation was assessed using an MTT assay. The results demonstrated that the upregulation of miR-19a-3p inhibited A549 and H1299 cell proliferation (Fig. 2B;  $P < 0.01$  and  $P < 0.001$ ). Furthermore, cells transfected with miR-19a-3p mimics exhibited significant attenuation in the ability to form colonies. The number of cell colonies formed by A549 cells transfected with miR-19a-3p mimics was reduced by 48.8% compared with miR-NC transfected cells (Fig. 2C;  $P < 0.001$ ).

**MiR-19a-3p overexpression suppresses cell migration and invasion in NSCLC.** Since miR-19a-3p was associated with lymph node metastasis in NSCLC specimens, the current study further assessed whether miR-19a-3p affects NSCLC cell migration and invasion. A wound healing assay was initially performed to determine the migratory ability of cells. As presented in Fig. 3A, a inhibited movement was observed in A549 and H1299 cells transfected with miR-19a-3p mimics compared with those transfected with miR-NC. Quantitative analysis further confirmed that the wound area in the miR-19a-3p group following 48 h culture was significantly decreased compared with miR-NC transfected A549 ( $P < 0.001$ ) and H1299 cells ( $P < 0.01$ ). Subsequently, a transwell Matrigel invasion assay was used to investigate the inhibitory effect of miR-19a-3p on the invasive potency of NSCLC cells. The results presented in Fig. 3B demonstrated that miR-19a-3p significantly suppressed A549 cell invasion by 87.0% (miR-NC vs. miR-19a-3p mimics;  $40.7 \pm 5.1$  vs.  $5.3 \pm 4.2$ ;  $P < 0.001$ ) and H1299 invasion by 81.1% (miR-NC vs. miR-19a-3p mimics;  $95.3 \pm 3.2$  vs.  $18.0 \pm 6.9$ ;  $P < 0.001$ ). These data further indicated that miR-19a-3p exerted an inhibitory effect on the migration and invasion of NSCLC cells.

**UBAP2L is a direct target of miR-19a-3p.** To assess the mechanism of miR-19a-3p on NSCLC progression, the potential target genes of miR-19a-3p were searched using online miRDB, miRanda and TargetScan databases. UBAP2L was selected as a potential target associated with NSCLC progression. As presented in Fig. 4A, the wild type and the mutant type binding site of miR-19a-3p with UBAP2L were identified. To confirm that UBAP2L was a direct target of miR-19a-3p, two recombinant expression vectors containing the 3'UTR of UBAP2L (UBAP2L WT) or its mutant version (UBAP2L MUT) were constructed and co-transfected with an miR-19a-3p mimic or miR-NC in A549 and H1299 cells. As presented in Fig. 4B, the luciferase activity assay demonstrated that transfection with the miR-19a-3p mimic significantly suppressed the luciferase activity of the wild type, and not mutant 3'UTR of UBAP2L in A549 ( $P < 0.01$ ) and H1299 cells ( $P < 0.001$ ). Furthermore, the expression of UBAP2L mRNA was significantly reduced in A549 ( $P < 0.01$ ) and H1299 ( $P < 0.001$ ) cells following transfection with miR-19a-3p mimics (Fig. 4C). In addition, upregulated miR-19a-3p inhibited UBAP2L protein expression in A549 and H1299 cells (Fig. 4D). These results suggested that UBAP2L is a target of miR-19a-3p in NSCLC cells.

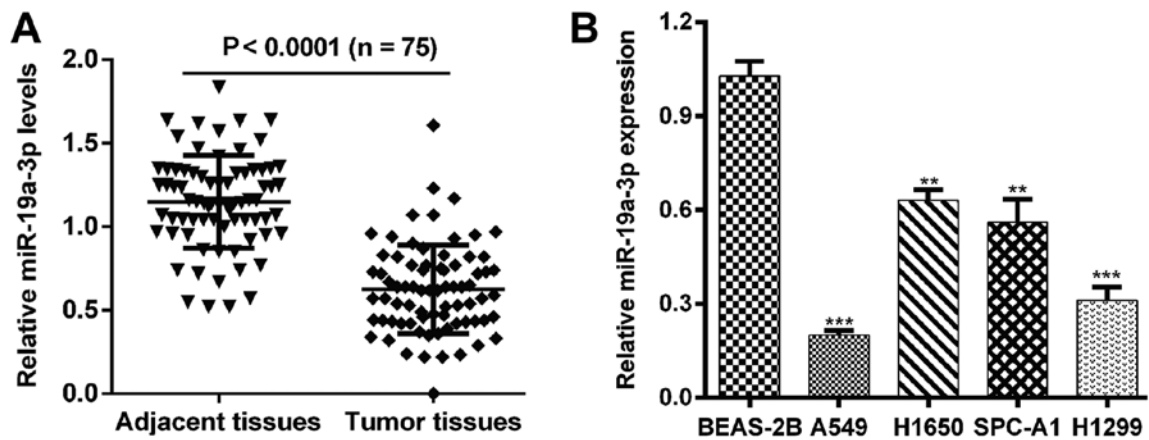


Figure 1. miR-19a-3p is downregulated in NSCLC tissues and cell lines. (A) RT-qPCR analysis of miR-19a-3p expression in 75 NSCLC tissues and adjacent noncancerous tissues. (B) The expression of miR-19a-3p in four NSCLC cell lines A549, H1650, SPC-A1 and H1299, compared with a human bronchial epithelial cell line BEAS-2B were detected using a RT-qPCR assay. \*\* $P < 0.01$  and \*\*\* $P < 0.001$  vs. BEAS-2B. MiR, miRNA; NSCLC, non-small cell lung cancer; miR, microRNA; RT-qPCR, reverse transcription-quantitative polymerase chain reaction.

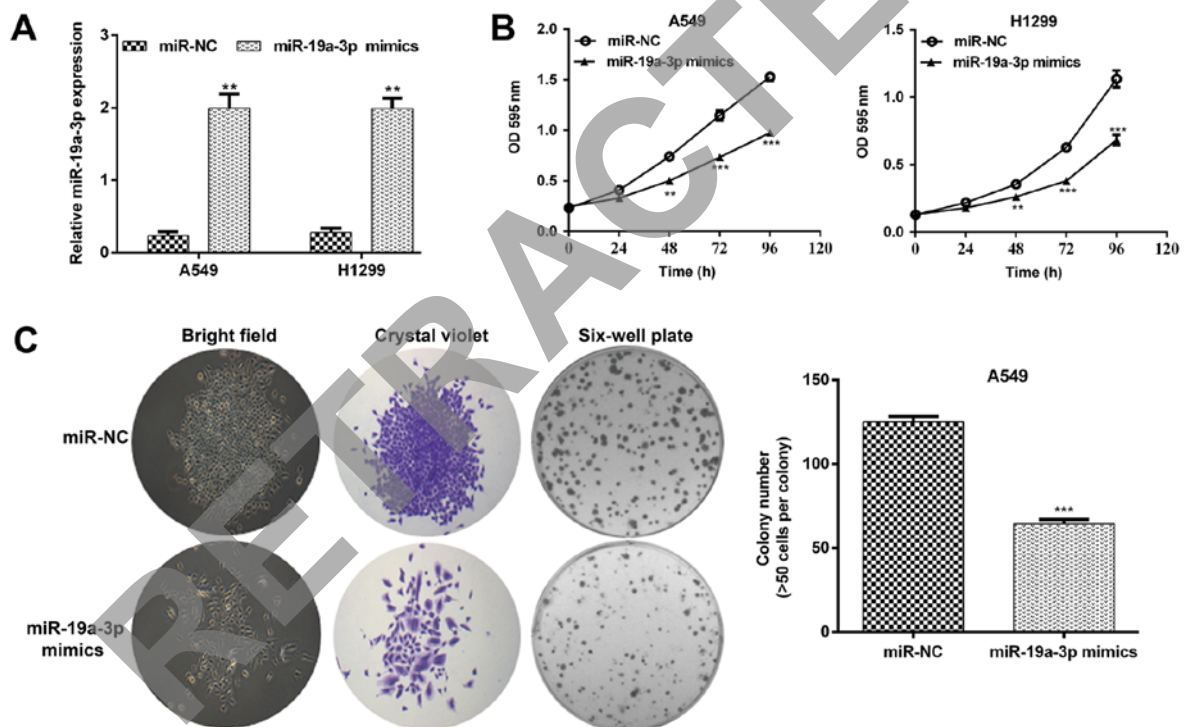


Figure 2. Elevated miR-19a-3p inhibited cell proliferation in NSCLC cells. A549 and H1299 cell lines were transfected with a miR-19a-3p mimic or miR-NC. (A) Quantitative analysis of miR-19a-3p levels in A549 and H1299 cell lines. (B) A549 and H1299 cell growth curves were measured using an MTT assay. (C) Representative images (left) and quantitative analysis (right) of A549 cell colony formation. Magnification,  $\times 200$ . Data are presented as the mean  $\pm$  standard deviation from triplicate experiments. \*\* $P < 0.01$  and \*\*\* $P < 0.001$  vs. miR-NC. NSCLC, non-small cell lung cancer; miR, miRNA; NC, negative control.

*Knockdown of UBAP2L suppresses cell proliferation, migration and invasion in NSCLC.* The expression of UBAP2L was determined using RT-qPCR and the association between miR-19a-3p and UBAP2L expression was also evaluated in NSCLC tissues. It was demonstrated that miR-19a-3p expression was inversely correlated with UBAP2L mRNA levels in NSCLC tissues (Fig. 5A;  $P = 0.0318$ ), indicating that UBAP2L may be an oncogene involved with the progression of NSCLC. Subsequently, a loss-of-function assay was performed to assess the functional role of UBAP2L in NSCLC cells. As presented in Fig. 5B, siUBAP2L transfection markedly downregulated

UBAP2L protein expression in A549 cells. An MTT assay further demonstrated that UBAP2L knockdown significantly suppressed the proliferation of A549 cells (Fig. 5C;  $P < 0.001$ ) at 72 and 96 h. Consistent with miR-19a-3p overexpression, UBAP2L knockdown significantly inhibited cell migration (Fig. 5D;  $P < 0.001$ ) and invasion (Fig. 5E;  $P < 0.01$ ) in A549 cells.

*UBAP2L upregulation partially reverses the suppressive effect of miR-19a-3p on NSCLC cell proliferation, migration and invasion.* To further confirm that the effects of miR-19a-3p



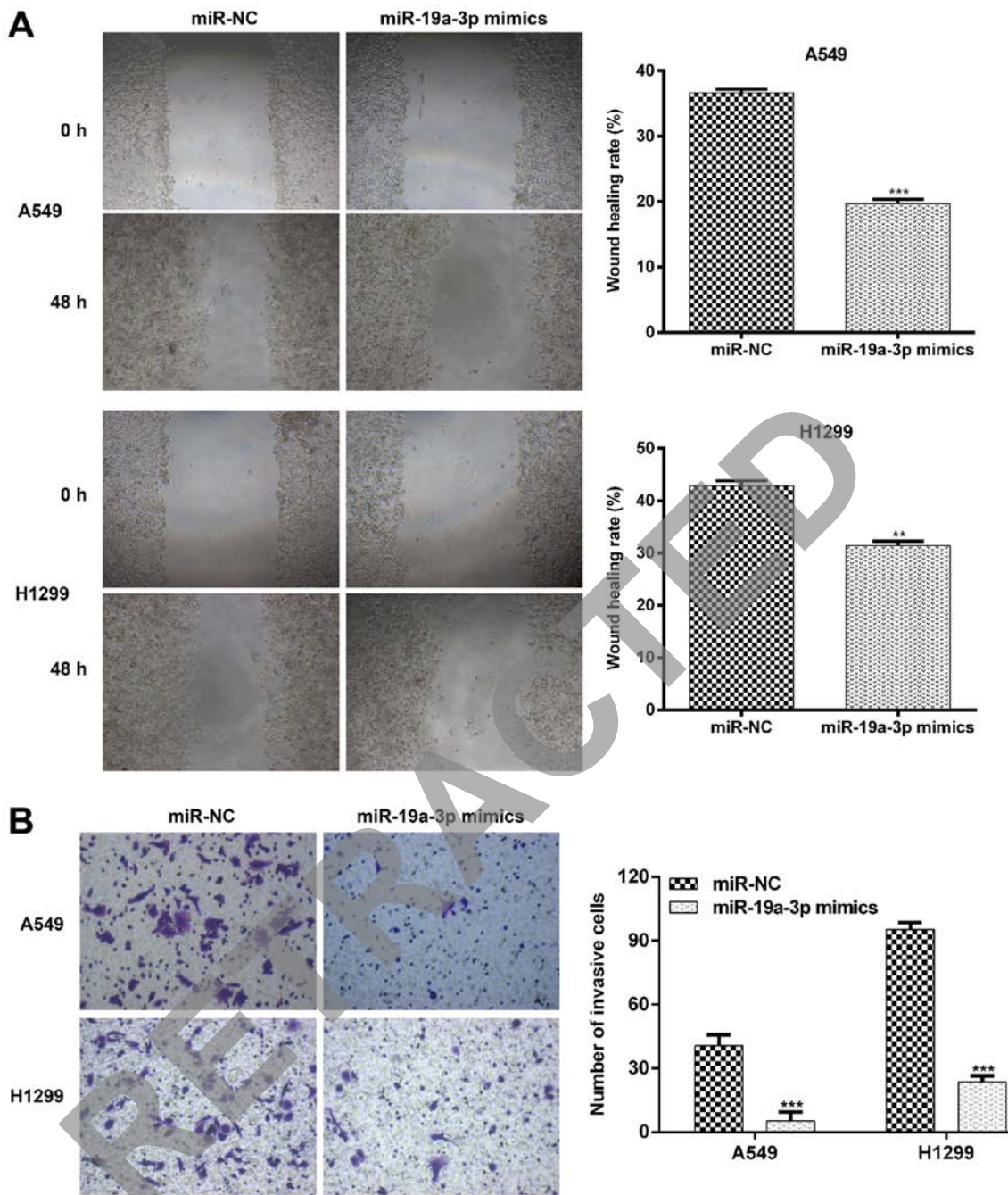


Figure 3. Elevated expression of miR-19a-3p suppressed NSCLC cell migration and invasion *in vitro*. (A) Wound healing assays were performed to assess the effect of miR-19a-3p on the migratory ability of A549 and H1299 cells. Images of the cells were obtained at 0 and 48 h. The relative migration length was established from three randomly selected locations. (B) The invasiveness of A549 and H1299 cells transfected with miR-19a-3p mimics or miR-NCs was examined using a transwell Matrigel invasion assay. Data are presented as the mean  $\pm$  standard deviation from triplicate experiments. \*\* $P < 0.01$  and \*\*\* $P < 0.001$  vs. miR-NC. NSCLC, non-small cell lung cancer; miR, miRNA; NC, negative control.

on NSCLC cell function are mediated by UBAP2L, rescue experiments were performed using A549 cells co-transfected with miR-19a-3p mimics, with or without the UBAP2L overexpression plasmid (pcDNA3.1-UBAP2L). As presented in Fig. 6A, UBAP2L protein levels were increased in A549 cells co-transfected with miR-19a-3p and pcDNA3.1-UBAP2L compared with those that were co-transfected with miR-19a-3p and the empty plasmid (pcDNA3.1). Furthermore, the MTT assay indicated that UBAP2L restoration in A549 cells significantly reversed the inhibition of cell proliferation by miR-19a-3p overexpression (Fig. 6B;  $P < 0.001$ ) at 72 and 96 h.

In addition, UBAP2L overexpression rescued impaired A549 cell migration and invasion, as determined by the wound healing (Fig. 6C;  $P < 0.001$ ) and transwell Matrigel invasion assays (Fig. 6D;  $P < 0.05$ ), respectively. Collectively, these results indicate that miR-19a-3p exerts its suppressive effect in NSCLC by directly inhibiting UBAP2L expression.

## Discussion

Evidence has suggested that the abnormal expression of certain miRNAs in NSCLC is associated with tumor development

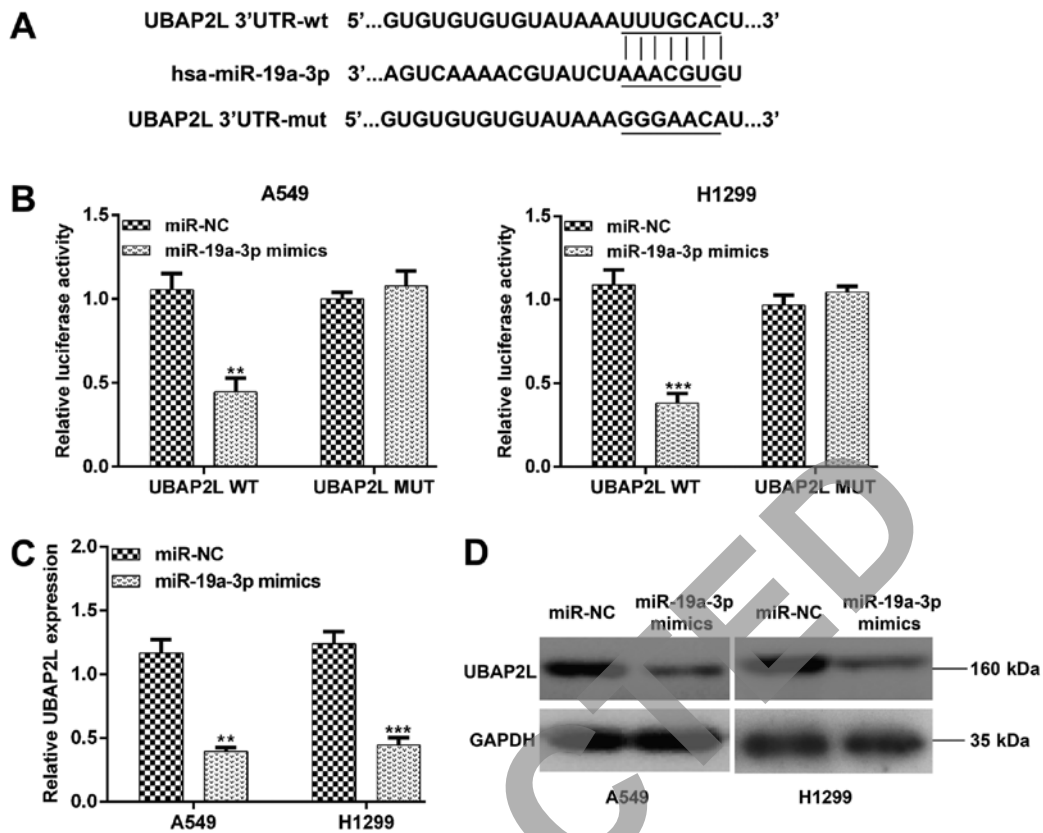


Figure 4. UBAP2L is a direct target of miR-19a-3p. (A) Schematic representation of the miR-19a-3p target sequence with the 3'-UTR of UBAP2L. The mutant 3'-UTR of UBAP2L is also presented. (B) A dual-luciferase reporter assay was performed using A549 and H1299 cells. (C) The expression of UBAP2L mRNA in A549 and H1299 cells transfected with miR-19a-3p mimics or miR-NC was detected using a reverse transcription-quantitative polymerase chain reaction assay. (D) UBAP2L protein levels were detected using Western blotting. Data are presented as the mean  $\pm$  standard deviation from triplicate experiments. \*\*P<0.01 and \*\*\*P<0.001 vs. miR-NC. UBAP2L, ubiquitin associated protein 2 like; UTR, untranslated region; miR, miRNA; NC, negative control; WT, wild type; MUT, mutant.

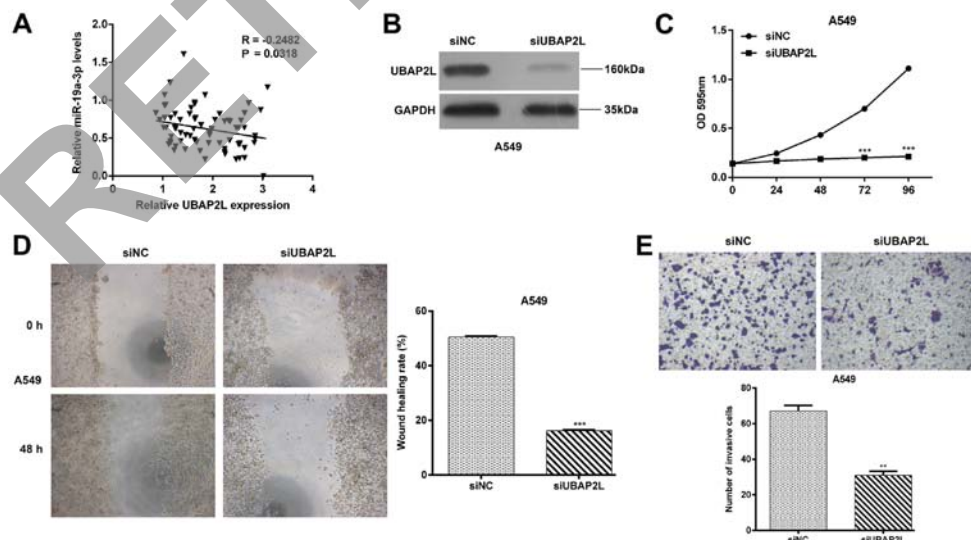


Figure 5. UBAP2L knockdown suppressed NSCLC cell proliferation, migration and invasion. (A) Pearson's correlation analysis was used to determine the association between miR-19a-3p and UBAP2L mRNA expression levels in NSCLC tissues. A549 cells were transfected with siUBAP2L or siNC for 48 h and (B) UBAP2L protein expression was determined by western blot analysis. (C) A549 cell proliferation was determined using an MTT assay. (D) Wound healing and (E) Transwell Matrigel invasion assays were performed to assess A549 cell migration and invasion. Data are presented as the mean  $\pm$  standard deviation from triplicate experiments. \*\*P<0.01 and \*\*\*P<0.001 vs. siNC. UBAP2L, ubiquitin associated protein 2 like; NSCLC, non-small cell lung cancer; miR, miRNA; si, small interfering; NC, negative control; OD, optical density.

and progression (24). Furthermore, a previous study demonstrated that miR-19a-3p downregulates the proto-oncogene

Fos-related antigen-1 to induce macrophage polarization and repress tumorigenesis and metastasis in breast cancer

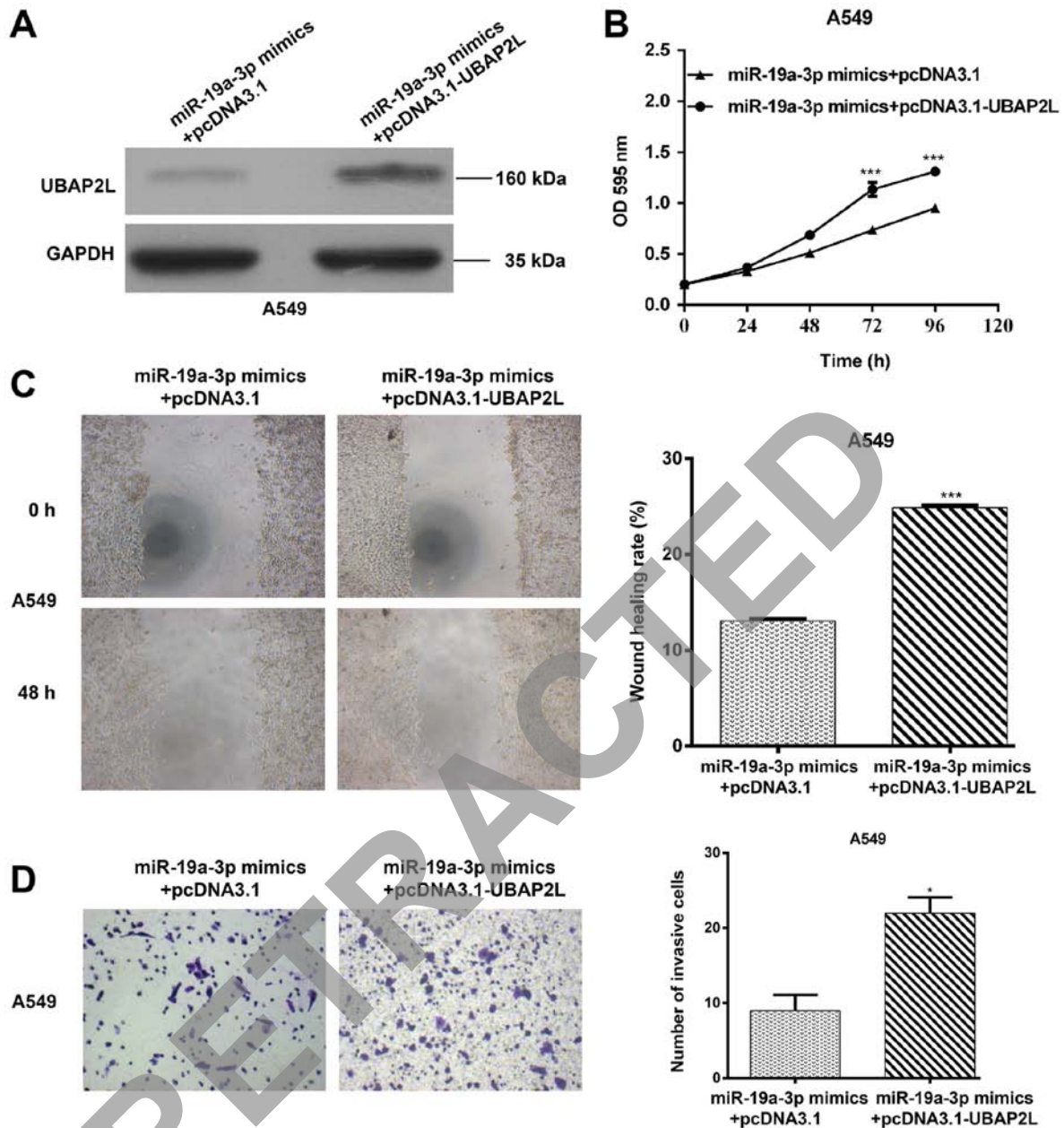


Figure 6. UBAP2L upregulation partially reverses the effects of miR-19a-3p on NSCLC cell proliferation, migration and invasion. A549 cells were transfected with pcDNA3.1 or pcDNA3.1 + UBAP2L expression plasmids, which in turn were co-transfected with the miR-19a-3p expression plasmid. (A) Western blotting was performed to assess UBAP2L protein expression. GAPDH was used as a loading control. (B) MTT, (C) wound healing and (D) Transwell Matrigel invasion assays were performed to determine A549 cell proliferation, migration and invasion. Data are presented as the mean  $\pm$  standard deviation from triplicate experiments. \* $P < 0.05$  and \*\*\* $P < 0.001$  vs. miR-19a-3p mimics + pcDNA3.1. UBAP2L, ubiquitin associated protein 2 like; miR, miRNA; NSCLC, non-small cell lung cancer; optical density.

cells (25). Zhang *et al* (14) revealed that elevating the expression of miR-19a-3p causes the upregulation of BCL2 and MDR mRNA and protein expression by targeting phosphatase and tensin homolog in myeloma. It was also demonstrated that miR-19a-3p facilitates the proliferation/invasion and impedes the apoptosis of myeloma cells (14). However, whether miR-19a-3p exerts similar effects on NSCLC cell malignant behavior remains unknown.

In the present study, it was revealed that miR-19a-3p was significantly decreased in NSCLC tissues and cell lines, and was associated with TNM stage and lymph node metastasis in patients with NSCLC. Additionally, the enhanced expression of miR-19a-3p inhibited NSCLC cell proliferation, colony

formation, invasion and migration by targeting UBAP2L. Previous studies have determined that miR-19a-3p serves as an oncogene in myeloma, but functions as an anti-oncogene in breast cancer and NSCLC (25,26). The current study hypothesized that tissue- and time-dependent expression of miR-19a-3p, along with the expression profiles of its target genes, may be responsible for these inconsistent results.

The luciferase reporter assay performed in the present study revealed the direct binding of miR-19a-3p to the 3'UTR of UBAP2L. Furthermore, miR-19a-3p negatively regulated UBAP2L in NSCLC A549 and H1299 cells. A previous study also revealed that the deficiency of UBAP2L in mouse embryos is associated with respiratory epithelium



disorganization during lung development (21). Additionally, UBAP2L has emerged as a regulator of epithelialization (21). Accumulating evidence has indicated that the disorganization and loss of epithelial polarity are hallmarks of epithelium during EMT (27). UBAP2L may also maintain the epithelial state of murine lung epithelial cells (21). In a previous study, the knockdown of UBAP2L resulted in decreased hepatocellular carcinoma cell EMT by regulating SNAIL1 (18). The present study demonstrated UBAP2L is a direct target of miR-19a-3p and that UBAP2L restoration markedly reversed the suppressive effects of cell proliferation, migration and invasion via miR-19a-3p overexpression. The current study therefore hypothesized that miR-19a-3p inhibited NSCLC A549 and H1299 cell invasion and migration by EMT through the downregulation of UBAP2L. Additionally, previous studies have demonstrated that UBAP2L knockdown inhibits prostate, breast and colorectal carcinoma cell proliferation (16,19,20), which is consistent with the results of the present study.

In conclusion, to the best of the authors' knowledge, this is the first study which demonstrates that miR-19a-3p is downregulated in NSCLC and that it is negatively correlated with the expression of UBAP2L, a novel target in NSCLC. Additionally, miR-19a-3p overexpression represses cell growth, invasion and migration in NSCLC cells by targeting UBAP2L. These results indicate that the upregulation and downregulation of miR-19a-3p and UBAP2L, respectively, may be a novel molecular target for the treatment of NSCLC.

#### Acknowledgements

Not applicable.

#### Funding

No funding was received.

#### Availability of data and materials

All data generated and/or analyzed during this study are available from the corresponding author on reasonable request.

#### Authors' contributions

HZ contributed to the conception and design of the research. YP and KJ contributed to the experiments and analysis of the data. XX and KW contributed to the analysis and interpretation of the data. All authors critically revised the manuscript, and agreed to be fully accountable for ensuring the integrity and accuracy of the work, and read and approved the final manuscript.

#### Ethics approval and consent to participate

The current study was approved by the Ethics Committee of Sun Yat-sen Memorial Hospital (Guangzhou, China).

#### Patient consent for publication

Not applicable.

#### Competing interests

The authors declare they have no competing interests.

#### References

1. Siegel RL, Miller KD and Jemal A: Cancer statistics, 2016. *CA Cancer J Clin* 66: 7-30, 2016.
2. Oser MG, Niederst MJ, Sequist LV and Engelman JA: Transformation from non-small-cell lung cancer to small-cell lung cancer: Molecular drivers and cells of origin. *Lancet Oncol* 16: e165-e172, 2015.
3. Peters S, Adjei AA, Gridelli C, Reck M, Kerr K, Felip E and ESMO Guidelines Working Group: Metastatic non-small-cell lung cancer (NSCLC): ESMO clinical practice guidelines for diagnosis, treatment and follow-up. *Ann Oncol* 23 (Suppl 7): vii56-vii64, 2012.
4. Osarogiagbon RU, Lin CC, Smeltzer MP and Jemal A: Prevalence, prognostic implications, and survival modulators of incompletely resected non-small cell lung cancer in the U.S. national cancer data base. *J Thorac Oncol* 11: e5-16, 2016.
5. Zinner R, Visseren-Gruij C, Spigel DR and Obasaju C: Pemetrexed clinical studies in performance status 2 patients with non-small cell lung cancer (Review). *Int J Oncol* 48: 13-27, 2016.
6. Chargar C, Deutsch E, Le Pechoux C and Magne N: State of the art in chemoradiotherapy combinations and potential role in targeting therapy approaches in nonsmall cell lung cancer. *Cancer Radiother* 13: 114-122, 2009 (In French).
7. Hafner M, Landgraf P, Ludwig J, Rice A, Ojo T, Lin C, Holoch D, Lim C and Tuschl T: Identification of microRNAs and other small regulatory RNAs using cDNA library sequencing. *Methods* 44: 3-12, 2008.
8. Pereira DM, Rodrigues PM, Borralho PM and Rodrigues CM: Delivering the promise of miRNA cancer therapeutics. *Drug Discov Today* 18: 282-289, 2013.
9. Wienholds E, Kloosterman WP, Miska E, Alvarez-Saavedra E, Berezikov E, de Bruijn E, Horvitz HR, Kauppinen S and Plasterk RH: MicroRNA expression in zebrafish embryonic development. *Science* 309: 310-311, 2005.
10. Dar AA, Majid S, de Semir D, Nosrati M, Bezrookove V and Kashani-Sabet M: miRNA-205 suppresses melanoma cell proliferation and induces senescence via regulation of E2F1 protein. *J Biol Chem* 286: 16606-16614, 2011.
11. Ambros V: MicroRNA pathways in flies and worms: Growth, death, fat, stress, and timing. *Cell* 113: 673-676, 2003.
12. Croce CM and Calin GA: miRNAs, cancer, and stem cell division. *Cell* 122: 6-7, 2005.
13. Wa Q, Li L, Lin H, Peng X, Ren D, Huang Y, He P and Huang S: Downregulation of miR19a3p promotes invasion, migration and bone metastasis via activating TGFbeta signaling in prostate cancer. *Oncol Rep* 39: 81-90, 2018.
14. Zhang X, Chen Y, Zhao P, Zang L, Zhang Z and Wang X: MicroRNA-19a functions as an oncogene by regulating PTEN/AKT/pAKT pathway in myeloma. *Leuk Lymphoma* 58: 932-940, 2017.
15. Maeda M, Hasegawa H, Sugiyama M, Hyodo T, Ito S, Chen D, Asano E, Masuda A, Hasegawa Y, Hamaguchi M and Senga T: Arginine methylation of ubiquitin-associated protein 2-like is required for the accurate distribution of chromosomes. *FASEB J* 30: 312-323, 2016.
16. Li D and Huang Y: Knockdown of ubiquitin associated protein 2-like inhibits the growth and migration of prostate cancer cells. *Oncol Rep* 32: 1578-1584, 2014.
17. Zhao B, Zong G, Xie Y, Li J, Wang H and Bian E: Downregulation of ubiquitin-associated protein 2-like with a short hairpin RNA inhibits human glioma cell growth in vitro. *Int J Mol Med* 36: 1012-1018, 2015.
18. Ye T, Xu J, Du L, Mo W, Liang Y and Xia J: Downregulation of UBAP2L inhibits the epithelial-mesenchymal transition via SNAIL1 regulation in hepatocellular carcinoma cells. *Cell Physiol Biochem* 41: 1584-1595, 2017.
19. He J, Chen Y, Cai L, Li Z and Guo X: UBAP2L silencing inhibits cell proliferation and G2/M phase transition in breast cancer. *Breast Cancer* 25: 224-232, 2018.
20. Chai R, Yu X, Tu S and Zheng B: Depletion of UBA protein 2-like protein inhibits growth and induces apoptosis of human colorectal carcinoma cells. *Tumour Biol* 37: 13225-13235, 2016.

21. Aucagne R, Girard S, Mayotte N, Lehnertz B, Lopes-Paciencia S, Gendron P, Boucher G, Chagraoui J and Sauvageau G: UBAP2L is amplified in a large subset of human lung adenocarcinoma and is critical for epithelial lung cell identity and tumor metastasis. *FASEB J* 31: 5012-5018, 2017.
22. Livak KJ and Schmittgen TD: Analysis of relative gene expression data using real-time quantitative PCR and the 2(-Delta Delta C(T)) method. *Methods* 25: 402-408, 2001.
23. Wang L, Jiang CF, Li DM, Ge X, Shi ZM, Li CY, Liu X, Yin Y, Zhen L, Liu LZ and Jiang BH: MicroRNA-497 inhibits tumor growth and increases chemosensitivity to 5-fluorouracil treatment by targeting KSR1. *Oncotarget* 7: 2660-2671, 2016.
24. Yu SL, Chen HY, Chang GC, Chen CY, Chen HW, Singh S, Cheng CL, Yu CJ, Lee YC, Chen HS, *et al*: MicroRNA signature predicts survival and relapse in lung cancer. *Cancer Cell* 13: 48-57, 2008.
25. Yang J, Zhang Z, Chen C, Liu Y, Si Q, Chuang TH, Li N, Gomez-Cabrero A, Reisfeld RA, Xiang R and Luo Y: MicroRNA-19a-3p inhibits breast cancer progression and metastasis by inducing macrophage polarization through down-regulated expression of Fra-1 proto-oncogene. *Oncogene* 33: 3014-3023, 2014.
26. Fan L, Sha J, Teng J, Li D, Wang C, Xia Q, Chen H, Su B and Qi H: Evaluation of serum paired MicroRNA ratios for differential diagnosis of Non-Small cell lung cancer and benign pulmonary diseases. *Mol Diagn Ther* 22: 493-502, 2018.
27. Heerboth S, Housman G, Leary M, Longacre M, Byler S, Lapinska K, Willbanks A and Sarkar S: EMT and tumor metastasis. *Clin Transl Med* 4: 6, 2015.

RETRACTED